Comparative DFT study on selective hydrogenation of acrolein catalyzed by pure Mo2C(001) and Pt/Mo2C(001)

Jinrong Wu
Xiangtan University

Yanping Huang (yph@xtu.edu.cn)
Xiangtan University https://orcid.org/0000-0002-6696-4916

Weiyan Wang
Xiangtan University

Wensong Li
Xiangtan University

Zhengke Li
Xiangtan University

Yunquan Yang
Xiangtan University

Research Article

Keywords: acrolein, selective hydrogenation, Mo2C(001), Pt/Mo2C(001), DFT

Posted Date: April 6th, 2021

DOI: https://doi.org/10.21203/rs.3.rs-255214/v1

Abstract

In this paper, Density Functional Theory (DFT) calculations were conducted to study the adsorption and stepwise hydrogenation of acrolein (CH 2 =CHCH=O) on pure Mo 2 C(001) and Pt/Mo 2 C(001). The electronic properties were investigated by Mulliken population analysis. The results showed that Mo atoms obtained some electrons from surrounding Pt and C atoms, thereby enhancing the hydrogenation activity of Mo atoms around Pt atoms and forming local active sites dominated by Mo atoms around Pt atoms. As a result, the adsorption energy of the species on Pt/Mo 2 C(001) is generally higher than that on Mo 2 C(001), and the activation energies of the elementary reactions involved in stepwise hydrogenation of acrolein on Pt/Mo 2 C(001) are lower than those on Mo 2 C(001). Moreover, Pt/Mo 2 C(001) exhibits higher selectivity for C=O bond hydrogenation than Mo 2 C(001) and produces more allyl alcohol.

1. Introduction

Recently, the selective hydrogenation of α, β-unsaturated aldehydes to produce corresponding unsaturated alcohols has attracted wide attention, because these unsaturated alcohols can be employed to produce valuable fine chemical and pharmaceutical intermediates and products[1, 2, 3, 4, 5, 6]. α, β-unsaturated aldehydes contain C=C bonds and C=O bonds. Generally, it is easier for C=C bonds to be hydrogenated than C=O bonds in thermodynamics and kinetics[7, 8, 9, 10, 11]. Therefore, we need to find a suitable catalyst to control the selectivity of hydrogenation, i.e., to improve the selectivity for C=O hydrogenation, so as to obtain the unsaturated alcohol required for production[12, 13, 14, 15].

Acrolein is the simplest α, β-unsaturated aldehyde with abundant sources. It can be formed by the decomposition of certain pollutants in the air or the incomplete combustion of organic matters, or as a metabolite in the human body. The electrophilic properties of acrolein play an important role in the reaction mechanism[16, 17]. Figure 1 is a reaction network of the selective hydrogenation of acrolein to propanol. There are four steps in total: the first step is to selectively hydrogenate C=O and C=C bonds to generate four intermediates; the second step is to add another hydrogen atom into the intermediates generated in the first step, forming propanal, enol and allyl alcohol, respectively; in the third step, four intermediates are generated via six routes; and in the fourth step, propanol is generated as the final hydrogenation product.

In the past research, Ir, Co, Pt, Ag and Ru are often used as catalysts to catalyze the hydrogenation of acrolein to unsaturated alcohols[18, 19, 20, 21, 22]. Luo et al.[23] studied the selective hydrogenation of acrolein to propanal on Ni(111). The selectivity of acrolein hydrogenation on Au(110), In/Au(110), Au_{20}, Au(211), Pt(211), Pt(111), Ag(110) and O_{sub}/Ag(111) was discussed. The results show that Pt is beneficial to the hydrogenation of C=O bond. In order to improve selectivity of the desired product, a second component can also be added to form a bimetallic catalyst. For example, such bimetallic catalysts as Ni/Pt(111), Pt/M(M=Ni, Co, Cu), Pt/Ni/Pt(111) and Pd/Ag(111) [24, 25, 26, 27] exhibit better

stability and activity. Such supported catalysts as Ag/TiO_2, Ag/SiO_2 and Au/ZnO[28, 29, 30] can be used to promote the interaction between components of the catalysts and fully expose the active centers.

Although precious metal materials exhibit great catalytic performance, they are expensive and short of resources. Transition metal carbides have received extensive attention because of their excellent physical and chemical properties, such as extremely high hardness, high melting point, excellent electrical conductivity and thermal conductivity. Among various transition metal carbides, Mo_2C not only has excellent catalytic activity, but also exhibits great resistance to CO and S poisoning and resistance to sintering[31]. It can be used as a low-cost catalyst to partially replace precious metal materials such as Pd and Pt. Rocha et al.[32] reported the theoretical and experimental studies on the continuous gas phase hydrogenation of benzene with bulk Mo_2C at 363 K. The results showed that the initial conversion rate of benzene to cyclohexane was 100%. However, the strong adsorption of benzene on the surface of Mo_2C will cause deactivation of the catalyst later. Shi et al.[33] reported the mechanism of the selective hydrogenation of furfural catalyzed by $Mo_2C(101)$ to methyl furan. Two schemes were proposed to promote the formation of methyl furan and inhibit the formation of furan. Frauwallner et al. [34] tested the catalytic activity of Mo_2C catalysts for toluene hydrogenation and the results showed that the catalytic activity of Mo_2C is equivalent to that of precious metals. Hollak et al.[35] compared activity, selectivity and stability of W_2C and Mo_2C catalysts supported by carbon nanofibers in oleic acid hydrodeoxygenation. The results showed that Mo_2C supported by carbon nanofibers showed higher activity and stability. Burueva et al.[36] reported that the phase composition of Mo_2C has a significant effect on the selectivity of stepwise hydrogenation. By changing the gas hourly space velocity of the carburizing gas mixture, a defective phase can be generated. The results showed that β-Mo_2C exhibited the best hydrogenation performance. Oliveira et al.[37] reported the mechanism of hydrodeoxygenation of acrylic acid on Mo_2C. The overall mechanism of the four-step reaction of acrylic acid to propane is proposed, and the main product is propane.

However, the mechanism of selective hydrogenation of acrolein on Mo_2C is still unclear. Wang et al. [38] used Density Functional Theory calculations to study the stability of the β-Mo_2C surface, and confirmed that the $Mo_2C(001)$ is the most stable at low temperatures and the surface is easily exposed. Under low carburizing ability, the surface with more molybdenum atoms is more stable. The $Mo_2C(001)$ is selected in this research because its structure is simple and it is the most densely filled surface, and it is expected to exist in a large amount on the nanostructured Mo_2C[39]. Therefore, in this study, the molybdenum-terminated $Mo_2C(001)$ surface was adopted as the catalyst model. The mechanism of selective hydrogenation of acrolein on $Mo_2C(001)$ and $Pt/Mo_2C(001)$ surface was studied by Density Functional Theory calculations.

2. Computational Models And Details

2.1 Computational surface models

Based on the optimized Mo_2C bulk structure, a $Mo_2C(001)$ surface model was built , using a 22 unit cell consisting of five layers of atoms with 15 Å of vacuum, as is shown in Figure 2a. The distance between adjacent C and Mo atoms in Figure 2a is between 2.08Å and 2.21Å, the distance between two adjacent C atoms and Mo atoms is 2.88Å. As shown in Figure 2b, the distance between the Pt atom and the adjacent Mo atom is 2.88 Å, and the distance between the Pt atom and the adjacent C atom is 2.05 Å. The two upmost surface layers and the adsorbates have been optimized, while the lowest three layers are kept fixed.

2.2 Computational details

Based on spin unrestricted DFT calculations conducted with DMol^3 in Materials Studio, the double numerical plus polarization (DNP) basis set was used in the calculations. The generalized gradient approximation (GGA) with the Perdew-Burke-Ernzerhoff (PBE) functional[40] was used as the exchange-correlation functional. A smearing of 0.005 Ha was adopted to accelerate the convergence. The k-point sampling consists of 221 Monkhorst-Pack points[41]. The convergence criteria for geometry optimization and energy calculations were set as 1.0×10^{-5} Ha, 2.0×10^{-5} Ha, 0.004 Ha/Å, and 0.005 Å for the tolerance of self-consistent field (SCF), energy, maximum force, and maximum displacement, respectively. Complete LST/QST[42] was used to identify the possible transition state(TS). The convergence criterion is the same as that of geometry optimization.

The adsorption energies of different species on $Mo_2C(001)$ and $Pt/Mo_2C(001)$ are defined as follows:

$E_{ads(A)}=E_{A/slab}-E_{slab}-Egas\ A$

Where $E_{A/slab}$, E_{slab} and Egas Arepresent the total energy of species A adsorbed on $Mo_2C(001)$ or $Pt/Mo_2C(001)$, the total energy of bare $Mo_2C(001)$ or $Pt/Mo_2C(001)$, and the total energy of species A in the vacuum.

The co-adsorption energies on $Mo_2C(001)$ and $Pt/Mo_2C(001)$ are defined as:

$E_{co\text{-}ads}=E_{(A+B)/slab}-Egas\ A-Egas\ B-E_{slab}$

Where $E_{(A+B)/slab}$, Egas A, Egas Band E_{slab} represent the total energy of species A and B co-adsorbed on the surface of $Mo_2C(001)$ or $Pt/Mo_2C(001)$, the total energy of species A in the vacuum, and the total energy of species B in the vacuum, the total energy of bare $Mo_2C(001)$ or $Pt/Mo_2C(001)$.

The activation energy of all elementary reactions is the total energy difference between the TS and the initial state (IS), as shown below:

$E_a=E_{TS}-E_{IS}$

The reaction energy is the total energy difference between the final state (FS) and the IS, as shown below:

$\Delta E=E_{FS}-E_{IS}$

3. Results And Discussion

For the convenience of description, as shown in Figure 1, the atoms of acrolein (CH_2=CHCH=O) are marked from left to right respectively as C1, C2, C3, O0, and the black dots indicate the lone electrons. On Mo_2C(001) and Pt/Mo_2C(001), acrolein is hydrogenated to allyl alcohol. In order to consider the formation of byproducts of the hydrogenation reaction, the reaction is divided into four steps, and the activation energy barriers each step need to overcome as well as the stable adsorption configuration and adsorption energy are analyzed.

3.1 Electronic properties

By studying the surface electronic properties of Mo_2C(001) and Pt/Mo_2C(001), we can better explain the electron transfer between Pt atoms and Mo_2C, and understand the synergetic effect between Pt and Mo_2C. Therefore, the Mulliken population of Mo_2C(001) and Pt/Mo_2C(001) was analyzed, and the results are shown in Figure 3. After Pt is added into Mo_2C(001), the electronegativity of the C atoms decreases, indicating that the C atoms lose electrons, while the electropositivity of the Mo atoms decreases, indicating that the Mo atoms gain electrons. The Pt atoms on the surface of Pt/Mo_2C(001) are positively charged, suggesting that the Pt atoms lose electrons, which demonstrates that both C atoms and Pt atoms transfer electrons to Mo atoms so that the Mo atoms around the Pt atoms on Pt/Mo_2C(001) have strong hydrogenation activity, which is beneficial to the hydrogenation reaction.

3.2 Adsorption on Mo_2C(001) and Pt/Mo_2C(001)

3.2.1 Single adsorption

The top view (top) and side view (bottom) of the adsorption structure of the substance involved in the hydrogenation of acrolein to propanol on Mo_2C (001) and Pt/Mo_2C (001) are shown in Figure 4 (top view and side view), and the adsorption energy is shown in Table 1.

Table 1 summarizes the corresponding adsorption energies of the aforementioned species on Mo_2C(001) and Pt/Mo_2C(001). Figure 4 shows the stable adsorption configurations of adsorbates on Mo_2C(001) and Pt/Mo_2C(001). It can be seen from Table 1 that the adsorption energies of almost all the species on Pt/Mo_2C(001) are larger than that on Mo_2C(001), which proves that the addition of Pt atoms onto Mo_2C(001) will enhance the interaction between the metal and most species. Binding strength of the adsorbate may be related to the transfer of electrons from Pt and C atoms to Mo atoms. It can be found from Figure 4 that when the adsorbate is on the surface of pure Mo_2C, the surface adsorption site is

mainly the top site of Mo atoms. C atoms only play a role of donating electrons and do not participate in the reaction. On Pt/Mo_2C(001), most adsorbates interact with the Pt atoms, and the active sites become the bridge sites of Pt and Mo. For example, on Pt/Mo_2C(001), H atoms tend to be adsorbed on the bridge sites between Pt atoms and Mo atoms. On Mo_2C(001), the most stable H adsorption site is the bridge site between two Mo atoms on the first layer. The stable adsorption sites of other adsorbates on Pt/Mo_2C(001) also involve Pt atoms and Mo atoms on the first layer. This may also explain the increase of the absolute value of the adsorption energy, because there is an extra active Pt atom to interact with the adsorbate, which also reduces the adsorption range of the adsorbed material and facilitates the selective hydrogenation.

Table 1 Calculated adsorption energy of each species on Mo_2C(001) and Pt/Mo_2C(001)

Species	Adsorption Energy (kcal/mol)	
	Mo_2C(001)	Pt/Mo_2C(001)
H	-67.08	-69.68
CH_2=CHCH=O	-64.63	-70.90
CH_3CHCH=O	-79.06	-77.81
CH_2CH_2CH=O	-76.49	-84.71
CH_2=CHCH_2O	-102.78	-102.85
CH_2=CHCHOH	-59.61	-72.16
CH_2=CHCH_2OH	-48.31	-48.43
CH_3CH_2CH=O	-39.53	-41.16
CH_3CH=CHOH	-37.65	-40.40
CH_3CH_2CHOH	-64.00	-64.55
$CH_3CH_2CH_2$O	-70.28	-73.62
CH_3CHCH_2OH	-71.53	-70.19
$CH_2CH_2CH_2$OH	-69.65	-69.68
$CH_3CH_2CH_2$OH	-25.10	-25.72

3.2.2 Co-adsorption

In this study, the co-adsorption of H atoms and various intermediates on $Mo_2C(001)$ and $Pt/Mo_2C(001)$ was studied. The comparisons of specific co-adsorption energies are shown in Table 2. The adsorption configuration is shown in Figure 5 (top view and side view). It can be seen that the addition of Pt onto $Mo_2C(001)$ increases the co-adsorption energy of almost all adsorbates, because the added Pt atoms have a strong binding strength with most species.

Table 2 Calculated co-adsorption energies on $Mo_2C(001)$ and $Pt/Mo_2C(001)$

Species	Adsorption Energy (kcal/mol)	
	$Mo_2C(001)$	$Pt/Mo_2C(001)$
CH_2=CHCH=O+H	-122.99	-140.62
CH_3CHCH=O+H	-138.05	-143.09
CH_2CH_2CH=O+H	-142.44	-155.18
CH_2=CHCH_2O+H	-173.19	-136.16
CH_2=CHCHOH+H	-112.95	-106.71
CH_2=CHCH_2OH+H	-104.79	-117.78
CH_3CH_2CH=O+H	-101.65	-104.25
CH_3CH=CHOH+H	-93.49	-106.08
$CH_2CH_2CH_2$OH+H	-128.64	-134.91
$CH_3CH_2CH_2$O+H	-143.64	-144.06
CH_3CH_2CHOH+H	-131.15	-136.16
CH_3CHCH_2OH+H	-131.15	-139.11

3.2.3 Changes in bond lengths

Table 3 summarizes the changes in bond lengths of each species on $Mo_2C(001)$ and $Pt/Mo_2C(001)$ during acrolein hydrogenation. It can be seen from Table 3 that the process of acrolein hydrogenation to propanol is a stretching process, and it can be seen from the table that the stretching degree of C=C bond is greater than that of C=O bond. The bond length of this site is obviously greater than that of other bonds at a larger distance. When the bond length of $Mo_2C(001)$ and $Pt/Mo_2C(001)$ changes, in general, the bond length on $Pt/Mo_2C(001)$ is smaller than the corresponding bond length on $Mo_2C(001)$. The bond

length stretch on the surface is smaller, probably because Mo seizes the electrons of the surrounding Pt and C atoms, which makes the binding strength of the adsorbate and Mo atoms stronger, so the bond length of the adsorption site on the Mo atom changes greatly, and the bond length change on the Pt site becomes smaller.

Table 3 Changes in bond length (Å) of species involved in acrolein hydrogenation on $Mo_2C(001)$ and $Pt/Mo_2C(001)$

Species	$Mo_2C(001)$			$Pt/Mo_2C(001)$		
	C1-C2	C2-C3	C3-O	C1-C2	C2-C3	C3-O
CH_2=CHCH=O	1.43	1.40	1.32	1.48	1.42	1.35
CH_3CHCH=O	1.50	1.39	1.34	1.42	1.46	1.39
CH_2CH_2CH=O	1.53	1.51	1.35	1.52	1.53	1.38
CH_2=CHCH_2O	1.39	1.51	1.42	1.49	1.53	1.42
CH_2CH=CHOH	1.40	1.40	1.44	1.46	1.41	1.43
CH_2=CHCH_2OH	1.42	1.49	1.48	1.42	1.46	1.50
CH_3CH_2CH=O	1.53	1.52	1.42	1.52	1.52	1.42
CH_3CH=CHOH	1.51	1.41	1.46	1.50	1.41	1.42
CH_3CH_2CHOH	1.53	1.51	1.50	1.52	1.52	1.41
$CH_3CH_2CH_2$O	1.52	1.52	1.40	1.51	1.51	1.48
CH_3CHCH_2OH	1.53	1.51	1.49	1.53	1.50	1.49
$CH_2CH_2CH_2$OH	1.54	1.51	1.47	1.50	1.52	1.47
$CH_3CH_2CH_2$OH	1.53	1.51	1.46	1.52	1.51	1.47

3.3 Elementary reactions on $Mo_2C(001)$ and $Pt/Mo_2C(001)$

From acrolein to propanol, the stepwise hydrogenation of acrolein was investigated to understand the hydrogenation of C=C and C=O bonds on $Pt/Mo_2C(001)$ and $Mo_2C(001)$, and the activation energy and reaction energy of each elementary reaction were calculated to analyze the kinetic and thermodynamic parameters in the acrolein hydrogenation. The negative value of the reaction energy indicates an exothermic reaction, while a positive value indicates an endothermic reaction. The specific values of the

activation energies and the reaction energies of the reaction are shown in Figures 6. The configurations of the transition states are shown in Figure 7.

Figure 6 shows the energy barriers of acrolein hydrogenation to propanol on $Mo_2C(001)$ and $Pt/Mo_2C(001)$. Figure 7 (top view on top, side view on bottom)shows the configurations of the transition states of elementary reactions. It can be seen from Figure 6 that the hydrogenation activity of acrolein on $Mo_2C(001)$ is lower than that on $Pt/Mo_2C(001)$. Next, the hydrogenation on the two catalyst surfaces will be compared.

The first step is that the H atom is added to acrolein to form four intermediates, i.e., $CH_3CHCH=O$, $CH_2CH_2CH=O$, $CH_2=CHCH_2O$ and $CH_2=CHCHO$. On $Mo_2C(001)$, the activation energy of the reaction is 63.10 kcal/mol, 30.01 kcal/mol, 63.92 kcal/mol and 58.288 kcal/mol, respectively. The reaction energy is -15.94 kcal/mol, 2.77 kcal/mol, -3.94 kcal/mol and 15.75 kcal/mol. On $Pt/Mo_2C(001)$, the activation energy is 37.44 kcal/mol, 27.36 kcal/mol, 24.59 kcal/mol and 10.05 kcal/mol, and the reaction energy is 7.17 kcal/mol, 15.18 kcal/mol, 7.27 kcal/mol and -27.59 kcal/mol. In the first step of acrolein hydrogenation, when hydrogenation occurs on $Mo_2C(001)$, C=C bond hydrogenation is easier than C=O bond hydrogenation. The most likely hydrogenation position is C2, because of its lowest energy barrier. On $Pt/Mo_2C(001)$, the activation energy barriers of the two hydrogenation sites of C=O are much lower than those of the two hydrogenation sites of C=C, i.e., $Pt/Mo_2C(001)$ has higher selectivity for C=O hydrogenation than $Mo_2C(001)$. Figure 8 shows energy profiles of the first hydrogenation step on $Pt/Mo_2C(001)$ (left) and $Mo_2C(001)$ (right) surfaces. R_n represents the reaction path, and the subscript n represents the C1, C2, C3 or O0 position. For example, R_1 represents hydrogenation of the C1 position, R_{12} represents hydrogenation of the C1 and C2 positions in sequence, and R_{123} represents hydrogenation of the C1, C2 and C3 positions in sequence. R_{1230} represents hydrogenation at positions C1, C2, C3 and O0 in sequence.

The second hydrogenation produces three important products, i.e., allyl alcohol ($CH_2=CHCH_2OH$), propanal ($CH_3CH_2CH=O$) and enol ($CH_3CH=CHOH$).

When the second H is added to the O0 position, the activation energy on the $Mo_2C(001)$ is 67.654 kcal/mol, and the allyl alcohol is hydrogenated at two positions (O0 and C3 positions) of the C=O bond. This is an endothermic reaction with an energy of 18.27 kcal/mol. On $Pt/Mo_2C(001)$, the reaction is an exothermic reaction, the energy barrier is reduced to 1.24 kcal/mol, and the reaction energy is -19.27 kcal/mol. The second possible way to form allyl alcohol is to add H atoms to C3. After searching the transition state, the activation energy of the reaction on the $Mo_2C(001)$ is 23.44 kcal/mol, and the reaction is exothermic by -18.37 kcal/mol. When Pt atoms are doped, the energy barrier becomes 44.07 kcal/mol, but the heat (-24.77 kcal/mol) released is slightly higher than that on $Mo_2C(001)$. The comparison results show that Pt doping can improve the selectivity for allyl alcohol.

Propanal ($CH_3CH_2CH=O$) is mainly produced by hydrogenation on the C=C bond. The hydrogenation of unsaturated aldehydes is most likely to produce saturated aldehydes. Therefore, when hydrogenating acrolein to produce allyl alcohol, the formation of saturated aldehyde (propanal) must be suppressed. The hydrogenation sites on acrolein are C1 and C2. When the C2 position is used as a hydrogenation site, the activation energy on $Mo_2C(001)$ is 19.78 kcal/mol and 67.78 kcal/mol, respectively, while the former is endothermic with the reaction energy of 1.16 kcal/mol, and the latter is exothermic by -6.94 kcal/mol. The energy barriers of two reactions on $Pt/Mo_2C(001)$ become 30.84 kcal/mol and 14.36 kcal/mol, respectively. The former is an endothermic reaction with an endothermic value of 3.47 kcal/mol, and the latter is an exothermic reaction with a heat release of -0.39 kcal/mol. The reaction occurs more easily on $Pt/Mo_2C(001)$ than on $Mo_2C(001)$.

The formation of enol ($CH_3CH=CHOH$) also has two hydrogenation sites. When H atom is added to the O0 site on $Mo_2C(001)$ and $Pt/Mo_2C(001)$, the activation energy barriers are 60.46 kcal/mol and 79.53 kcal/mol. The reaction energy of the endothermic reaction is 16.01 kcal/mol and 19.36 kcal/mol. When H atom is added to C1 position on $Mo_2C(001)$ and $Pt/Mo_2C(001)$, the activation energy of the reaction is 68.17 kcal/mol and 61.59 kcal/mol, and the reaction energy is -11.18 kcal/mol and -24.99 kcal/mol. Since the enol ($CH_3CH=CHOH$) itself is unstable, the calculation is only to make the data more complete.

To sum up, among the three products generated from acrolein, i.e., allyl alcohol ($CH_2=CHCH_2OH$), propanal ($CH_3CH_2CH=O$) and enol ($CH_3CH=CHOH$), hydrogenation on $Pt/Mo_2C(001)$ is easier than that on $Mo_2C(001)$, and on $Pt/Mo_2C(001)$, the selectivity for allyl alcohol is obviously greater than that of propanal. The most likely route for producing allyl alcohol is $CH_2=CHCH=O \rightarrow CH_2=CHCH_2O \rightarrow CH_2=CHCH_2OH$, and the most probable route for generating propanal ($CH_3CH_2CH=O$) is $CH_2=CHCH=O \rightarrow CH_2CH_2CH=O \rightarrow CH_3CH_2CH=O$. On the surface of $Pt/Mo_2C(001)$ and $Mo_2C(001)$, a higher activation energy barrier needs to be overcome to generate enol ($CH_3CH=CHOH$), so the reaction is not easy to occur. The C=C hydrogenation of acrolein on $Mo_2C(001)$ has high selectivity, but it is only conducive to the production of C2 hydrogenation product $CH_2CH_2CH=O$, which is not conducive to the production of the desired target product allyl alcohol. Figure 9 shows the energy barrier diagram of the second step reaction. The results show that the upper energy barrier of Pt/Mo_2C (001) is significantly reduced.

The third step was investigated in order to examine the stability of several products of acrolein hydrogenation, i.e., allyl alcohol and propanal. To make the data more complete, enol hydrogenation was also further investigated. The third step hydrogenation formed four intermediates, $CH_3CH_2CH_2O$, CH_3CH_2CHOH, CH_3CHCH_2OH and $CH_2CH_2CH_2OH$. Only by hydrogenation at the C3 position of propanal can the intermediate $CH_3CH_2CH_2O$ be obtained. On $Pt/Mo_2C(001)$ and $Mo_2C(001)$, the reaction energy barriers are 24.44 kcal/mol and 77.30 kcal/mol, respectively. The former has an endothermic value of 11.67 kcal/mol, and the latter reaction is exothermic by -1.66 kcal/mol. When propanal is hydrogenated

at the O0 position, CH_3CH_2CHOH is generated. During hydrogenation on Pt/Mo_2C(001) and Mo_2C(001), the reaction activation energies are 72.74 kcal/mol and 54.20 kcal/mol, and the reaction is endothermic by 10.20 kcal/mol and 5.43 kcal/mol, respectively. The results show that Pt/Mo_2C(001) is more beneficial to the hydrogenation of propanal than the Mo_2C(001), and the most favorable hydrogenation position is C3.

Allyl alcohol has two hydrogenation positions, i.e., C1 hydrogenation and C2 hydrogenation, to form CH_3CHCH_2OH and $CH_2CH_2CH_2OH$, respectively. When the C1 position is hydrogenated, the activation energy is 83.46 kcal/mol and 21.11 kcal/mol on Pt/Mo_2C(001) and Mo_2C(001), respectively. The reaction on Pt/Mo_2C(001) is an endothermic reaction with an endothermic value of 2.83 kcal/mol, while on Mo_2C(001) it is exothermic by -11.23 kcal/mol. As for C2 hydrogenation, the activation energies on Pt/Mo_2C(001) and Mo_2C(001) are 80.19 kcal/mol and 77.10 kcal/mol, respectively. The former is an endothermic reaction with the reaction energy of 7.43 kcal/mol. The latter reaction is exothermic with the reaction energy of -6.62 kcal/mol. The results show that Pt addition is not conducive to the hydrogenation of allyl alcohol, which means that the target product, allyl alcohol, is relatively stable.

There are two positions for hydrogenation of enol ($CH_3CHCHOH$). When CH_3CH_2CHOH and CH_3CHCH_2OH are generated on Pt/Mo_2C(001), the activation energies are 41.23 kcal/mol and 72.83 kcal/mol, while on Mo_2C(001) the activation energies are 18.00 kcal/mol and 71.44 kcal/mol. On Pt/Mo_2C(001) the reaction energies are -0.16 kcal/mol and -0.14 kcal/mol, while on Mo_2C(001) the reaction energies are -13.50 kcal/mol and -6.62 kcal/mol. The results show that enols are more prone to hydrogenation reaction on Mo_2C(001) than on Pt/Mo_2C(001). Figure 10 shows the energy change of each path during the third step of hydrogenation.

The fourth hydrogenation product is propanol ($CH_3CH_2CH_2OH$), which can be formed by hydrogenation of four intermediates, i.e., $CH_3CH_2CH_2O$, CH_3CH_2CHOH, CH_3CHCH_2OH and $CH_2CH_2CH_2OH$, respectively by adding H atoms to O0, C3, C2 and C1. As can be seen from Figures 6, it is not easy to produce propanol on Mo_2C(001), but on Pt/Mo_2C(001), it can be obtained by hydrogenation of two intermediates ($CH_3CH_2CH_2O$ and CH_3CH_2CHOH), and the corresponding activation energies are respectively 20.67 kcal/mol and 30.56 kcal/mol. The reaction energies are 18.44 kcal/mol and 8.95 kcal/mol, respectively. Since CH_3CH_2CHOH is difficult to obtain, propanol mainly derives from C=C bond hydrogenation. In general, the main products of acrolein hydrogenation are allyl alcohol and propanol. And the selectivity for allyl alcohol is higher than that of propanol. Figure 11 shows energy profiles of the forth hydrogenation step on Pt/Mo_2C(001) (left) and Mo_2C(001) (right) surfaces.

4. Conclusions

The adsorption energy and co-adsorption energy of most species on Pt/Mo_2C(001) are greater than that on Mo_2C(001), showing that the addition of Pt atoms enhances the interaction between most species and metal atoms on Pt/Mo_2C(001). It is found through electronic analysis that adding Pt atoms will transfer the electrons of Pt and C atoms to Mo atoms, and Mo atoms will gain more electrons, so the Mo atoms around Pt have stronger hydrogenation activity. Almost all the adsorbates are adsorbed on Mo atoms around Pt atoms with greater adsorption energies.

In order to further study the selectivity of hydrogenation of C=C and C=O bonds on Pt/Mo_2C(001) and Mo_2C(001), a comprehensive investigation of acrolein hydrogenation on Pt/Mo_2C(001) and Mo_2C(001) was conducted. The results show that the hydrogenation reaction of C=C on Mo_2C(001) is easier than that of C=O bond. The hydrogenation of C2 position is easier, but propanal cannot be easily obtained because the hydrogenation of intermediate CH_2CH_2CH=O needs to overcome a higher energy barrier. The energy barrier of hydrogenation of C=O bonds on the Pt/Mo_2C(001) is obviously lower than that of hydrogenation of C=C bonds, indicating that Pt/Mo_2C(001) is beneficial to improve the selectivity for C=O bonds. And with further calculations, it is found that the target product, allyl alcohol, is not prone to further hydrogenation, while propanal is prone to further hydrogenation to propanol. Therefore, the most likely products produced by acrolein hydrogenation on Pt/Mo_2C(001) are allyl alcohol and propanol, and the allyl alcohol selectivity is higher than that of propanol.

Declarations

Funding: This research was supported by the National Natural Science Foundation of China (No. 21676225 (Yunquan Yang) and 21776236(Weiyan Wang)), Natural Science Foundation of Hunan Province (2018JJ2384(Weiyan Wang)).

Conflicts of interest/Competing interests: **No**

Availability of data and material: N/A

Code availability: N/A

Authors' contributions: Jinrong Wu: Investigation, Data curation, Writing-Original draft preparation. Yanping Huang: Conceptualization, Methodology, Writing - review & editing. Weiyan Wang: Supervision, Funding acquisition. Wensong Li: Writing - review & editing. Zhengke Li: Writing - review & editing. Yunquan Yang: Resources, Supervision, Funding acquisition.

References

[1] A. Daimon, T. Kamitanaka, N. Kishida, T. Matsuda and T. Harada. Selective reduction of unsaturated aldehydes to unsaturated alcohols using supercritical 2-propanol. The Journal of Supercritical Fluids. 2006, 37(2): 215-219.

[2] H. Sundén, I. Ibrahem and A. Córdova. Direct organocatalytic asymmetric epoxidation of α,β-unsaturated aldehydes. Tetrahedron Letters. 2006, 47(1): 99-103.

[3] B.-C. Hong, H.-C. Tseng and S.-H. Chen. Synthesis of aromatic aldehydes by organocatalytic [4+2] and [3+3] cycloaddition of α,β-unsaturated aldehydes. Tetrahedron. 2007, 63(13): 2840-2850.

[4] J. Gogoi, P. Gogoi, P. Bezbaruah and R. C. Boruah. Microwave-assisted Pd-catalyzed synthesis of fused steroidal and non-steroidal pyrimidines from β-halo-α,β-unsaturated aldehydes. Tetrahedron Letters. 2013, 54(52): 7136-7139.

[5] S. Arimitsu, M. Oshiro and T. Yonamine. A new umpolung for direct γ-regioselective nucleophilic addition of alcohols to γ-enolizable α,β-unsaturated aldehydes. Tetrahedron Letters. 2017, 58(25): 2517-2520.

[6] Pengyu Lia, Liwei Mia, Yuanyuan Liub, Wenqin Zhang, Xian-Lei Shi. Synergistic catalysis of bifunctional polyacrylonitrile fiber for the synthesis of (E)-α,β-unsaturated esters from aldehydes by decarboxylative Doebner–Knoevenagel reaction. Journal of Industrial and Engineering Chemistry. 2020, 81: 323–331.

[7] Bo, Yang, Dong, Wang, Xue-Qing, Gong and H. J. P. C. C. P. Pccp. Acrolein hydrogenation on Pt(211) and Au(211) surfaces: a density functional theory study. 2011.

[8] Z. M. R. Wen Qiang Du, Yan Liang, Yong Wang, Xin Yi Lu, Yi Fan Wang, Lian Hai Lu. Chemoselective hydrogenation of a,b-unsaturated aldehydes with modified Pd/C catalyst. Chinese Chemical Letters. 2012, 23: 773–776.

[9] D. Giziński, I. Goszewska, M. Zieliński, D. Lisovytskiy, K. Nikiforov, J. Masternak, M. Zienkiewicz-Machnik, A. Śrębowata and J. Sá. Chemoselective flow hydrogenation of α,β – Unsaturated aldehyde with nano-nickel. Catalysis Communications. 2017, 98: 17-21.

[10] A. S. Rocha, L. A. Souza, R. R. Oliveira, A. B. Rocha and V. Teixeira da Silva. Hydrodeoxygenation of acrylic acid using Mo2C/Al2O3. Applied Catalysis A: General. 2017, 531: 69-78.

[11] X. Wang, Y. He, Y. Liu, J. Park and X. Liang. Atomic layer deposited Pt-Co bimetallic catalysts for selective hydrogenation of α, β-unsaturated aldehydes to unsaturated alcohols. Journal of Catalysis. 2018, 366: 61-69.

[12] D. Loffreda, F. Delbecq, F. Vigne and P. Sautet. Fast prediction of selectivity in heterogeneous catalysis from extended Bronsted-Evans-Polanyi relations: a theoretical insight. Angew Chem Int Ed Engl. 2009, 48(47): 8978-8980.

[13] D. A. Esan and M. Trenary. Surface chemistry of propanal, 2-propenol, and 1-propanol on Ru(001). Physical Chemistry Chemical Physics. 2017, 19(17): 10870-10877.

[14] W. Wan, S. C. Ammal, Z. Lin, K. E. You, A. Heyden and J. G. Chen. Controlling reaction pathways of selective C-O bond cleavage of glycerol. Nat Commun. 2018, 9(1): 4612.

[15] Y. Zhou, Z. Li, Y. Liu, J. Huo, C. Chen, Q. Li, S. Niu and S. Wang. Regulating Hydrogenation Chemoselectivity of alpha,beta-Unsaturated Aldehydes by Combination of Transfer and Catalytic Hydrogenation. Chemsuschem. 2020, 13(7): 1746-1750.

[16] G.-J. Kang, J. Ma and Z.-X. Chen. Theoretical Studies of Species Related to Acrolein Hydrogenation. Catalysis Letters. 2012, 142(2): 287-293.

[17] O. G. Salnikov, K. V. Kovtunov, D. A. Barskiy, A. K. Khudorozhkov, E. A. Inozemtseva, I. P. Prosvirin, V. I. Bukhtiyarov and I. V. Koptyug. Evaluation of the Mechanism of Heterogeneous Hydrogenation of alpha,beta-Unsaturated Carbonyl Compounds via Pairwise Hydrogen Addition. ACS Catalysis. 2014, 4(6): 2022-2028.

[18] H. Wei, C. Gomez, J. Liu, N. Guo, T. Wu, R. Lobo-Lapidus, C. L. Marshall, J. T. Miller and R. J. Meyer. Selective hydrogenation of acrolein on supported silver catalysts: A kinetics study of particle size effects. Journal of Catalysis. 2013, 298: 18-26.

[19] Y. Huang, X. Dong, Y. Yu and M. Zhang. The influence of surface oxygen and hydroxyl groups on the dehydrogenation of ethylene, acetic acid and hydrogenated vinyl acetate on pure Pd(1 0 0): A DFT study. Applied Surface Science. 2016, 388, Part A: 455-460.

[20] D. A. Esan, Y. Ren, X. Feng and M. Trenary. Adsorption and Hydrogenation of Acrolein on Ru(001). The Journal of Physical Chemistry C. 2017, 121(8): 4384-4392.

[21] D. A. Esan and M. Trenary. Selective Hydrogenation of Acrolein to Propanal on a Pseudomorphic Pt/Ru(001) Bimetallic Surface. Topics in Catalysis. 2018, 61(5-6): 318-327.

[22] W. B. Gong, M. M. Han, C. Chen, Y. Lin, G. H. Wang, H. M. Zhang and H. J. Zhao. CoOx@Co Nanoparticle-based Catalyst for Efficient Selective Transfer Hydrogenation of alpha,beta-Unsaturated Aldehydes. Chemcatchem. 2020, 12(4): 1019-1024.

[23] Q. Luo, T. Wang, M. Beller and H. Jiao. Acrolein Hydrogenation on Ni(111). The Journal of Physical Chemistry C. 2013, 117(24): 12715-12724.

[24] L. E. Murillo, A. M. Goda and J. G. Chen. Selective hydrogenation of the C=O bond in acrolein through the architecture of bimetallic surface structures. J Am Chem Soc. 2007, 129(22): 7101-7105.

[25] L. E. Murillo, C. A. Menning and J. G. Chen. Trend in the CC and CO bond hydrogenation of acrolein on Pt–M (M=Ni, Co, Cu) bimetallic surfaces. Journal of Catalysis. 2009, 268(2): 335-342.

[26] M. Trenary. Spectroscopic characterization of the structure and reaction pathways of Pd-Cu(111) and Pd-Ag(111) single-atom alloys. Abstracts of Papers of the American Chemical Society. 2019, 258.

[27] Y. Meng, S. Xia, X. Zhou and G. Pan. Mechanism of selective hydrogenation of cinnamaldehyde on Ni-Pt(111) with different structures: A comparative study. Chemical Physics Letters. 2020, 740.

[28] C. Volckmar, M. Bron, U. Bentrup, A. Martin and P. Claus. Influence of the support composition on the hydrogenation of acrolein over Ag/SiO2–Al2O3 catalysts. Journal of Catalysis. 2009, 261(1): 1-8.

[29] A. Ulgen and W. F. Hoelderich. Conversion of glycerol to acrolein in the presence of WO3/TiO2 catalysts. Applied Catalysis a-General. 2011, 400(1-2): 34-38.

[30] Z. Li, W.-P. Ding, G.-J. Kang and Z.-X. Chen. Hydrogen-mediated support effects on acrolein hydrogenation over ZnO supported gold clusters. Catalysis Communications. 2012, 17: 164-167.

[31] D. Fu, W. Guo, Y. Liu and Y. Chi. Adsorption and dissociation of H2S on Mo2C(001) surface-A first-principle study. Applied Surface Science. 2015, 351: 125-134.

[32] A. S. Rocha, A. B. Rocha and V. T. da Silva. Benzene adsorption on Mo2C: A theoretical and experimental study. Applied Catalysis A: General. 2010, 379(1-2): 54-60.

[33] Y. Shi, Y. Yang, Y.-W. Li and H. Jiao. Mechanisms of Mo2C(101)-Catalyzed Furfural Selective Hydrodeoxygenation to 2-Methylfuran from Computation. ACS Catalysis. 2016, 6(10): 6790-6803.

[34] M.-L. Frauwallner, F. López-Linares, J. Lara-Romero, C. E. Scott, V. Ali, E. Hernández and P. Pereira-Almao. Toluene hydrogenation at low temperature using a molybdenum carbide catalyst. Applied Catalysis A: General. 2011, 394(1-2): 62-70.

[35] S. A. W. Hollak, R. W. Gosselink, D. S. van Es and J. H. Bitter. Comparison of Tungsten and Molybdenum Carbide Catalysts for the Hydrodeoxygenation of Oleic Acid. ACS Catalysis. 2013, 3(12): 2837-2844.

[36] D. B. Burueva, A. A. Smirnov, O. A. Bulavchenko, I. P. Prosvirin, E. Y. Gerasimov, V. A. Yakovlev, K. V. Kovtunov and I. V. Koptyug. Pairwise Parahydrogen Addition Over Molybdenum Carbide Catalysts. Topics in Catalysis. 2019, 63(1-2): 2-11.

[37] R. R. Oliveira and A. B. Rocha. Acrylic acid hydrodeoxygenation reaction mechanism over molybdenum carbide studied by DFT calculations. J Mol Model. 2019, 25(10): 309.

[38] T. Wang, X. Liu, S. Wang, C. Huo, Y.-W. Li, J. Wang and H. Jiao. Stability of β-Mo2C Facets from ab Initio Atomistic Thermodynamics. The Journal of Physical Chemistry C. 2011, 115(45): 22360-22368.

[39] J. W. Han, L. Li and D. S. Sholl. Density Functional Theory Study of H and CO Adsorption on Alkali-Promoted Mo2C Surfaces. The Journal of Physical Chemistry C. 2011, 115(14): 6870-6876.

[40] B. Hammer, L. B. Hansen and J. K. Nørskov. Improved adsorption energetics within density-functional theory using revised Perdew-Burke-Ernzerhof functionals. Physical Review B. 1999, 59(11): 7413-7421.

[41] H. J. Monkhorst and J. D. Pack. Special points for Brillouin-zone integrations. Physical Review B. 1976, 13(12): 5188-5192.

[42] N. Govind, M. Petersen, G. Fitzgerald, D. King-Smith and J. Andzelm. A generalized synchronous transit method for transition state location. Computational Materials Science. 2003, 28(2): 250-258.

Figures

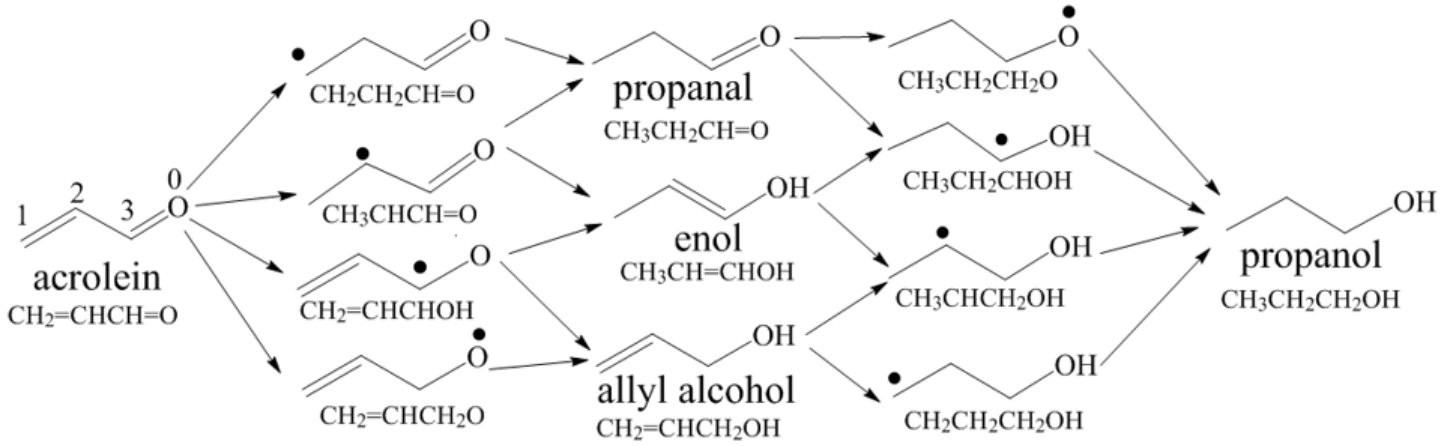

Figure 1

Reaction network of acrolein hydrogenation: Black dots indicate the lone electron.

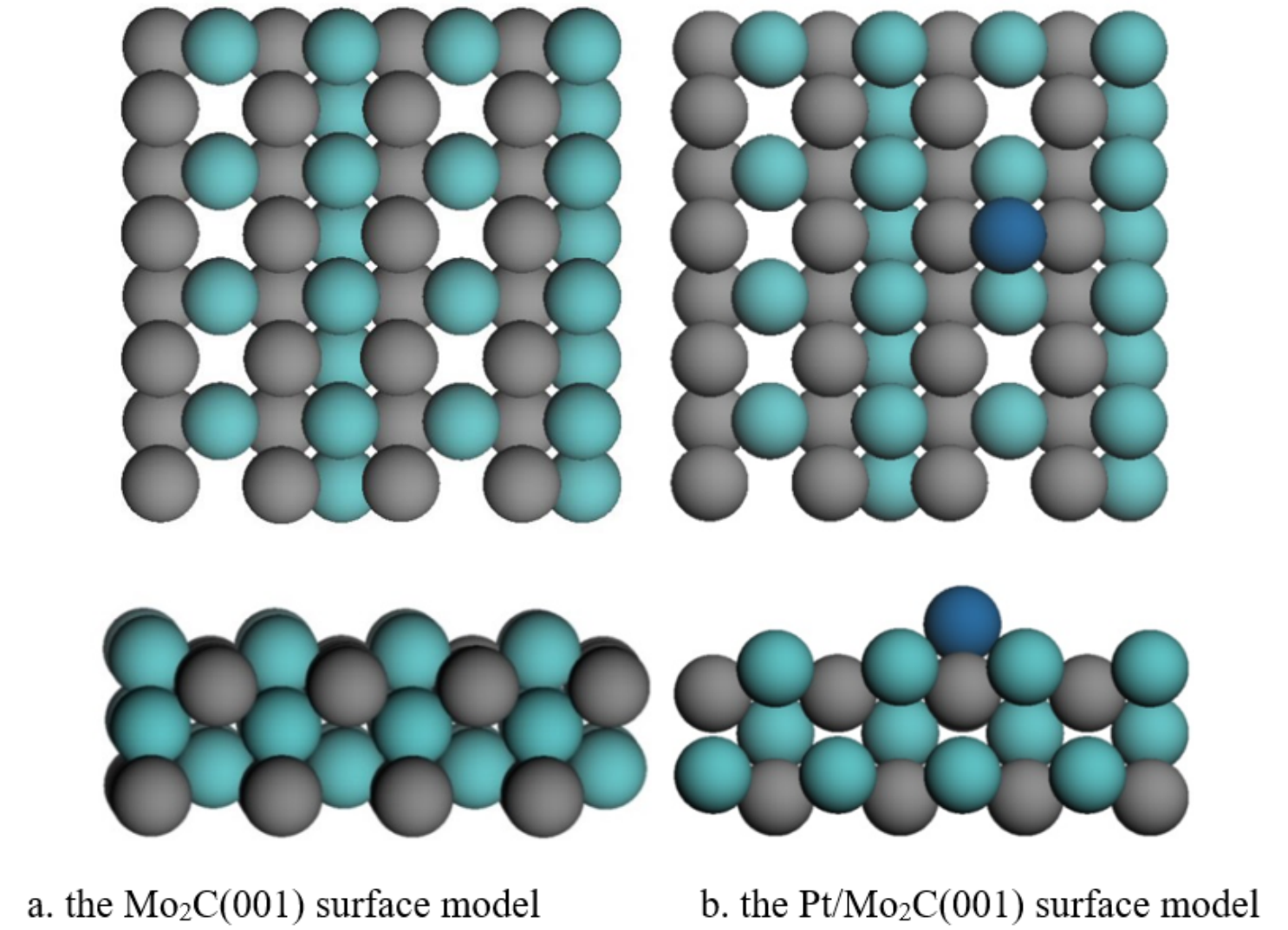

Figure 2

the Mo2C(001) surface model and the Pt/Mo2C(001) surface model (deep blue balls represent Pt atoms, gray balls represent C atoms, and light blue balls represent Mo atoms)

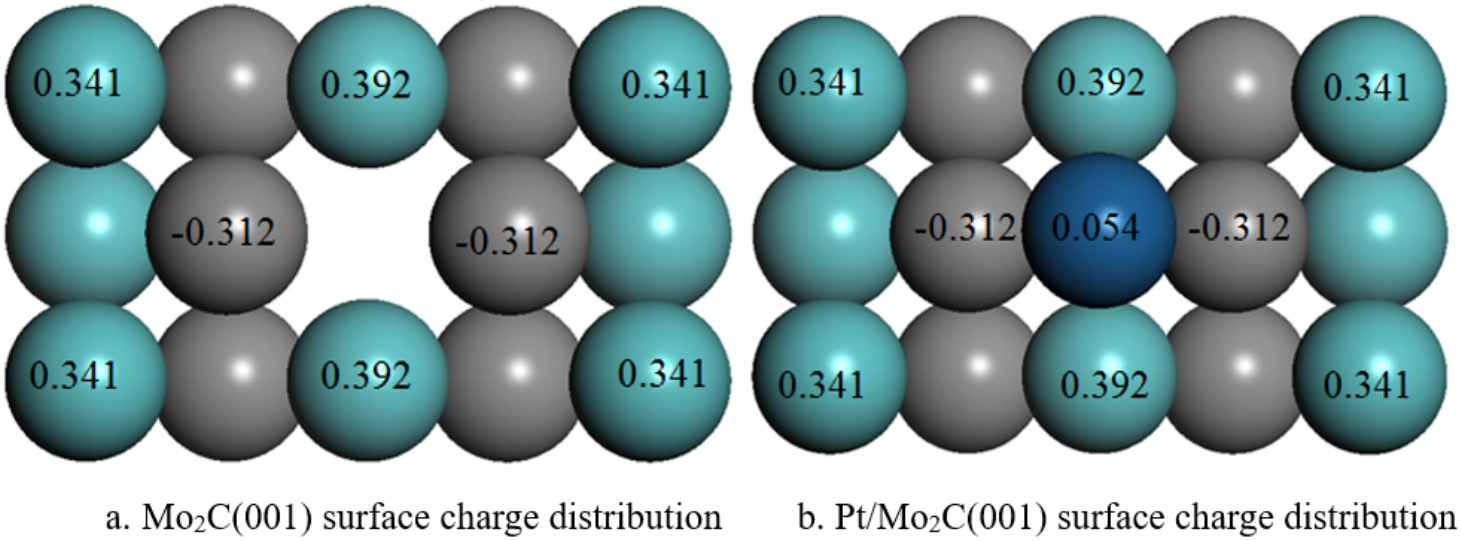

Figure 3

charge distribution of Mo2C(001) and Pt/Mo2C(001) (gray balls represent C atoms, blue-green balls represent Mo atoms, and the blue ball represents the Pt atom; balls with numbers are the surface atoms while those without numbers are atoms on the second layer)

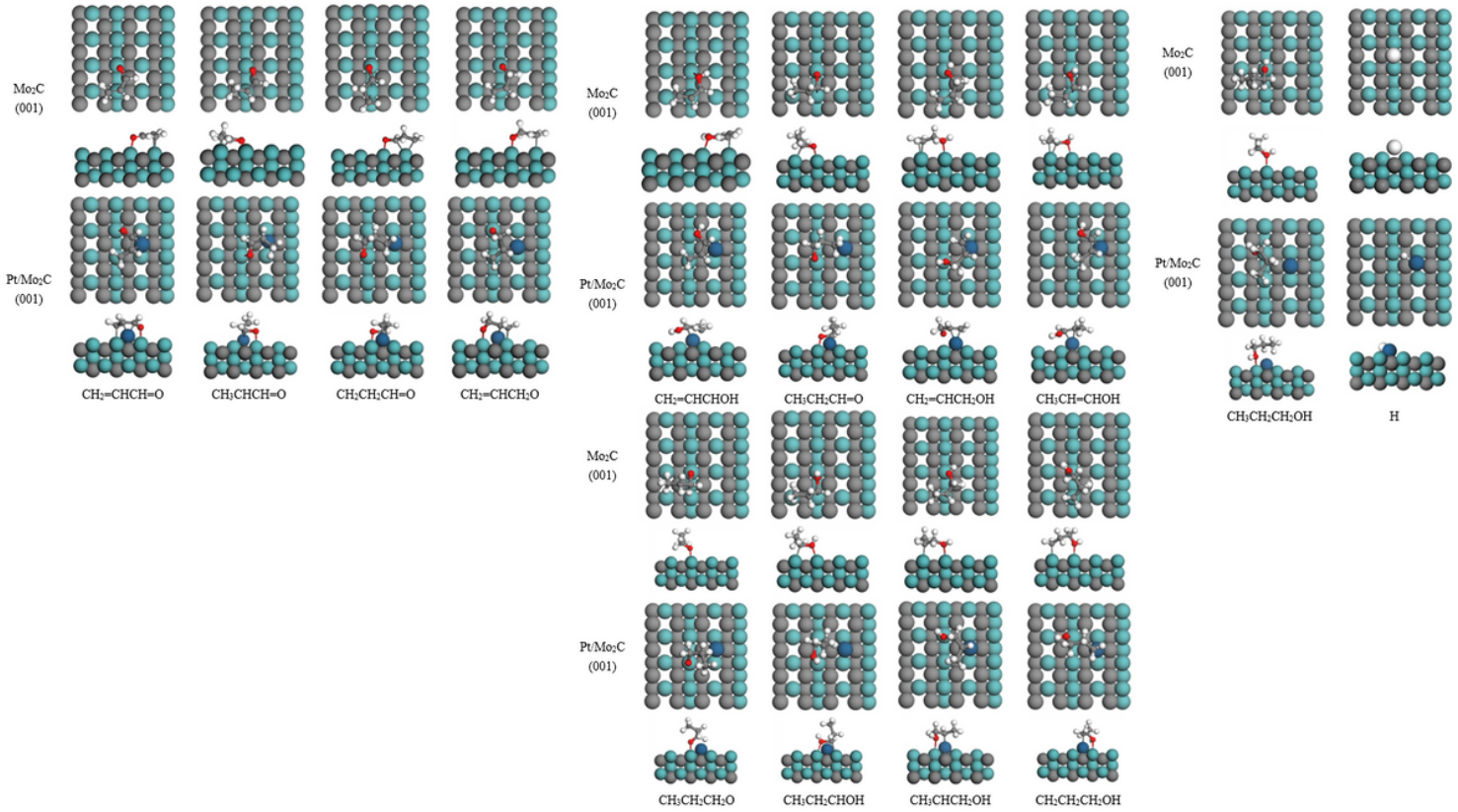

Figure 4

The stable adsorption configurations of species involved in acrolein hydrogenation to propanol on Mo2C(001) and Pt/Mo2C(001). (Red balls represent O atoms, and white balls represent H atoms)

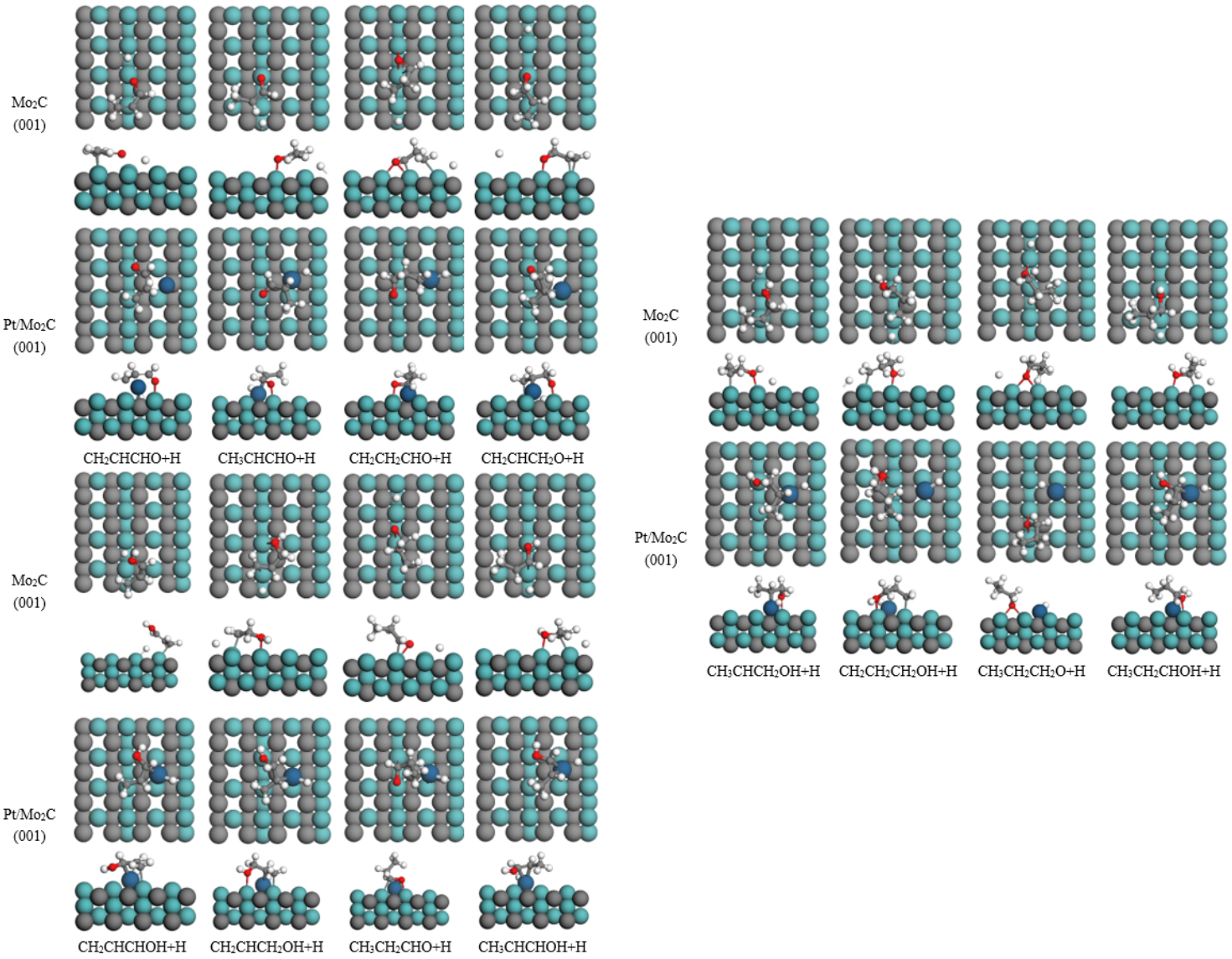

Figure 5

Co-adsorption configuration of species involved in acrolein hydrogenation to propanol on Mo2C(001) and Pt/Mo2C(001)

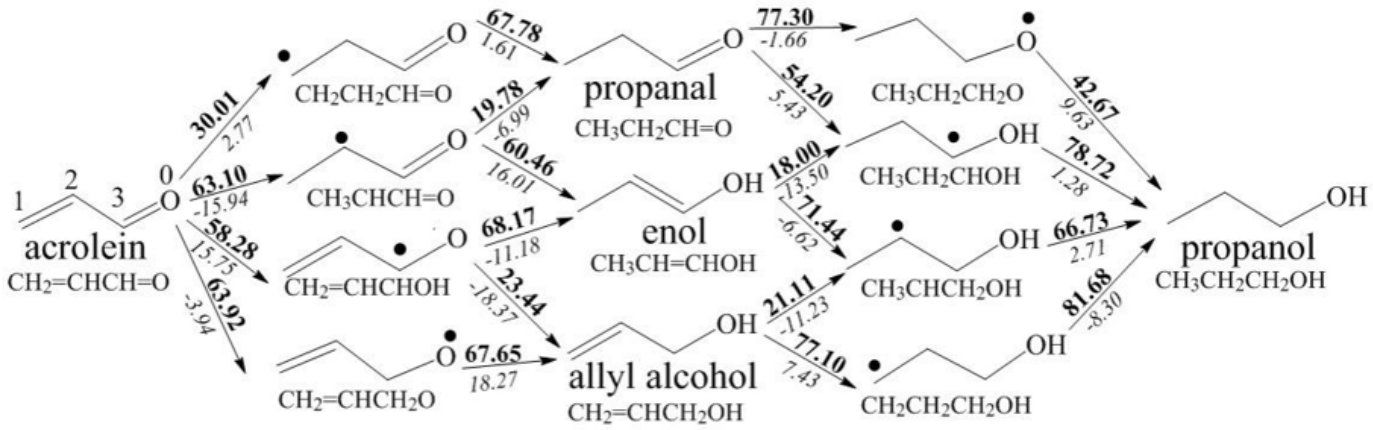

a. the activation energy (E_a) and reaction energy (ΔE) of each elementary reaction of acrolein hydrogenation on $Mo_2C(001)$

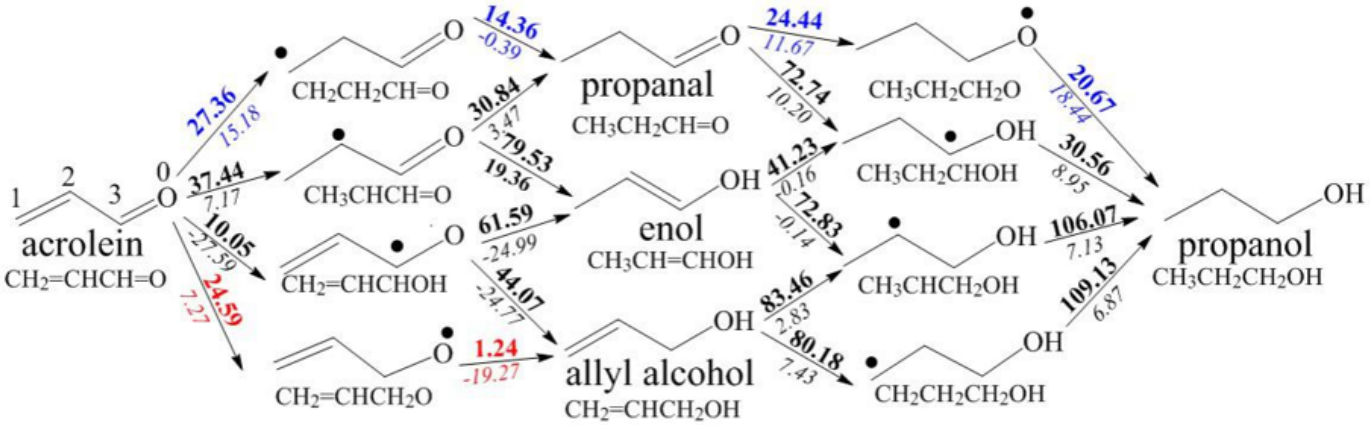

b. the activation energy (E_a) and reaction energy (ΔE) of each elementary reaction of acrolein hydrogenation on $Pt/Mo_2C(001)$

Figure 6

the activation energy (Ea) and reaction energy (ΔE) of each elementary reaction of acrolein hydrogenation on Pt/Mo2C(001) and Pt/Mo2C(001) (red is the most probable production route for allyl alcohol, blue is the most probable production route for propanol, and italics are reaction energies, bold numbers are activation energies. The unit is kcal/mol.)

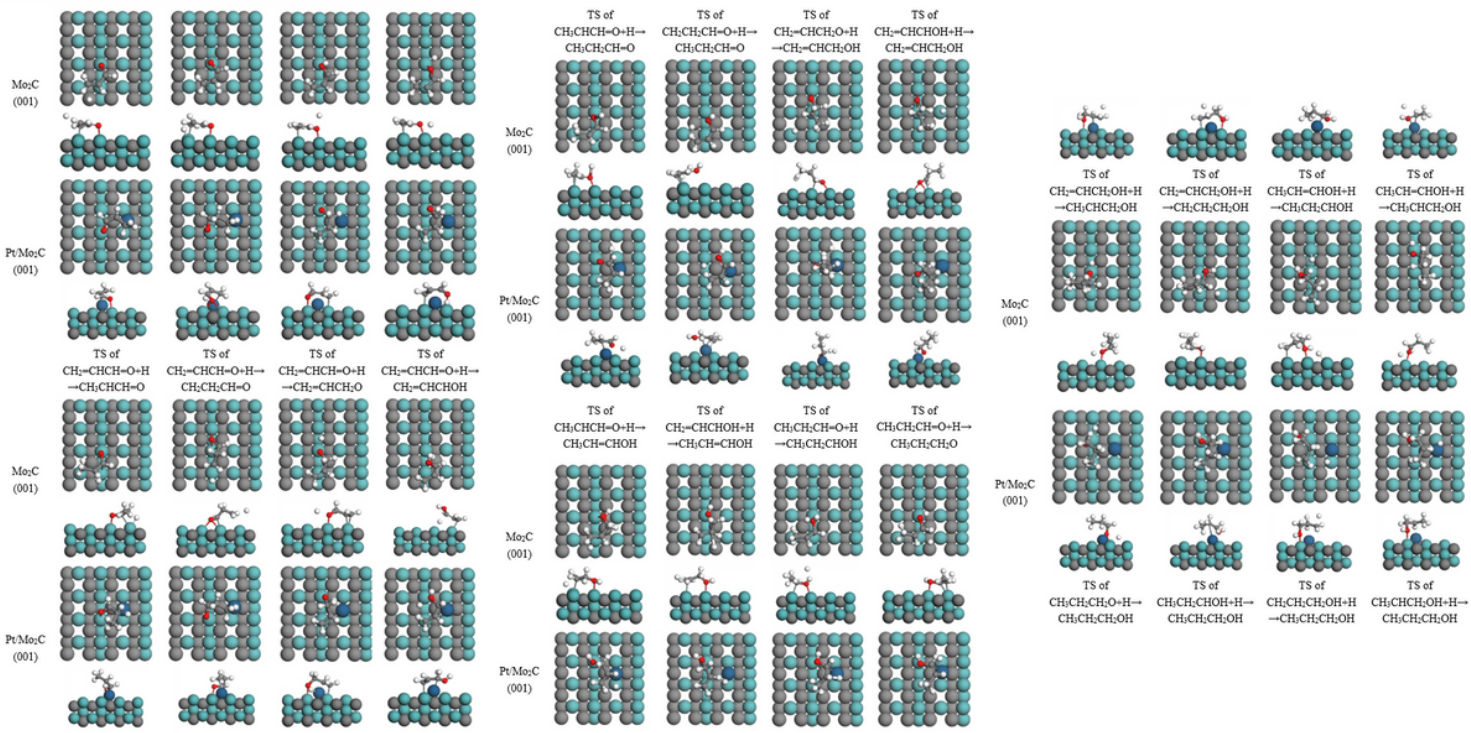

Figure 7

Transition states of elementary reactions of acrolein hydrogenation on Mo2C(001) and Pt/Mo2C(001)

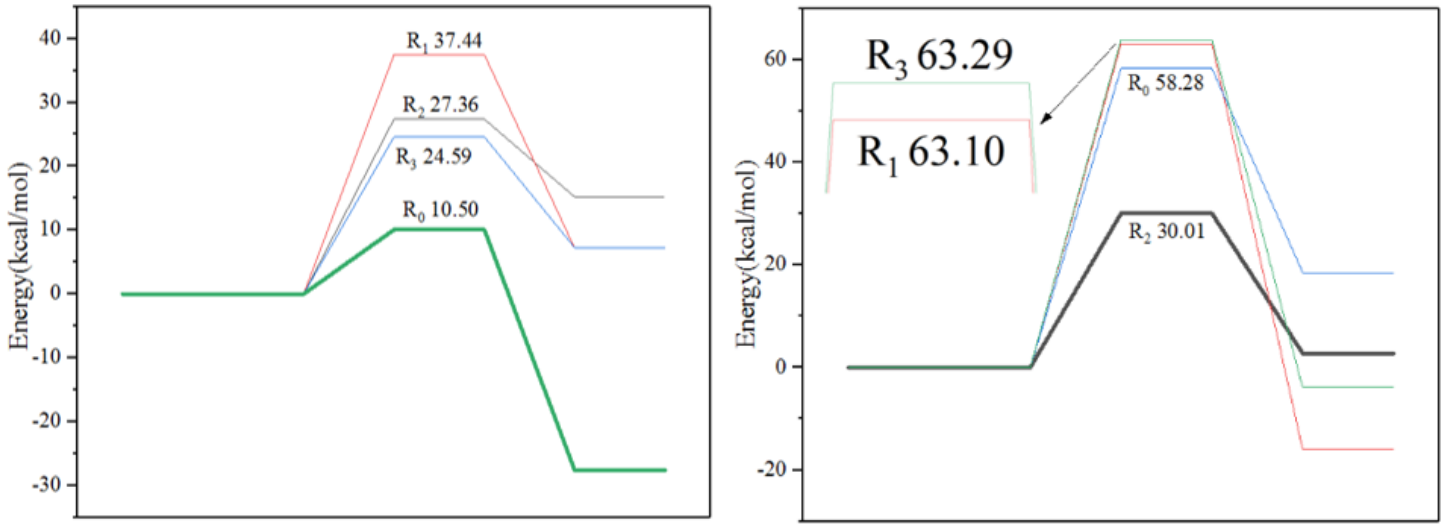

Figure 8

Energy profiles of the first hydrogenation step on Pt/Mo2C(001) (left) and Mo2C(001) (right) surfaces

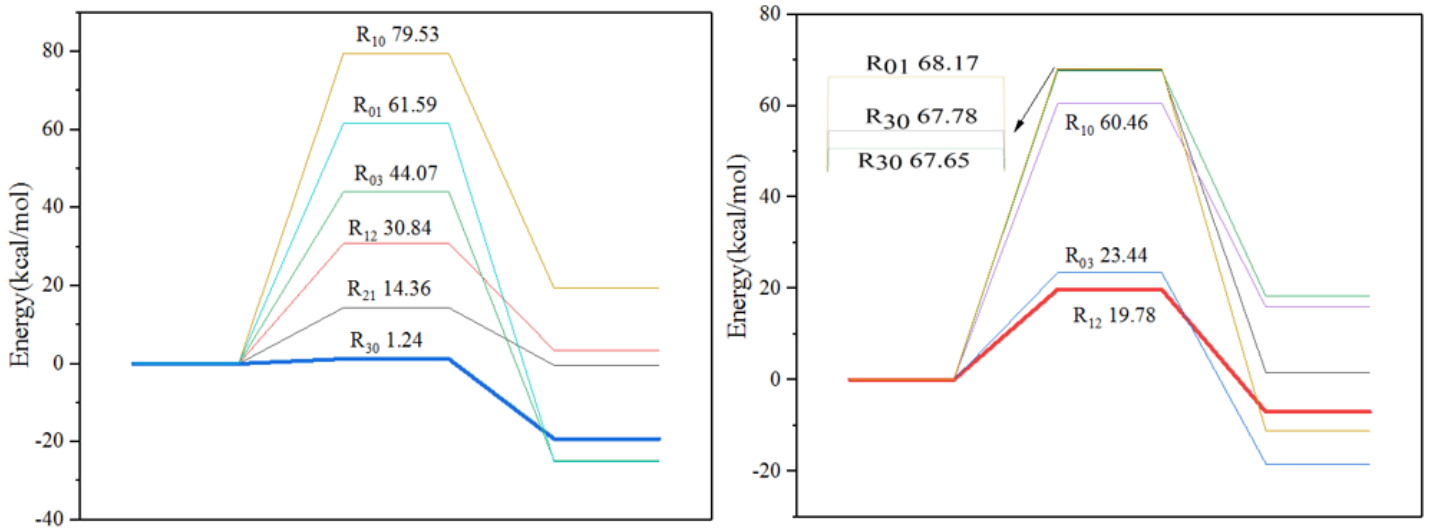

Figure 9

The energy distribution of the second step hydrogenation reaction on the surface of Pt/Mo2C (001) (left) and Mo2C (001) (right)

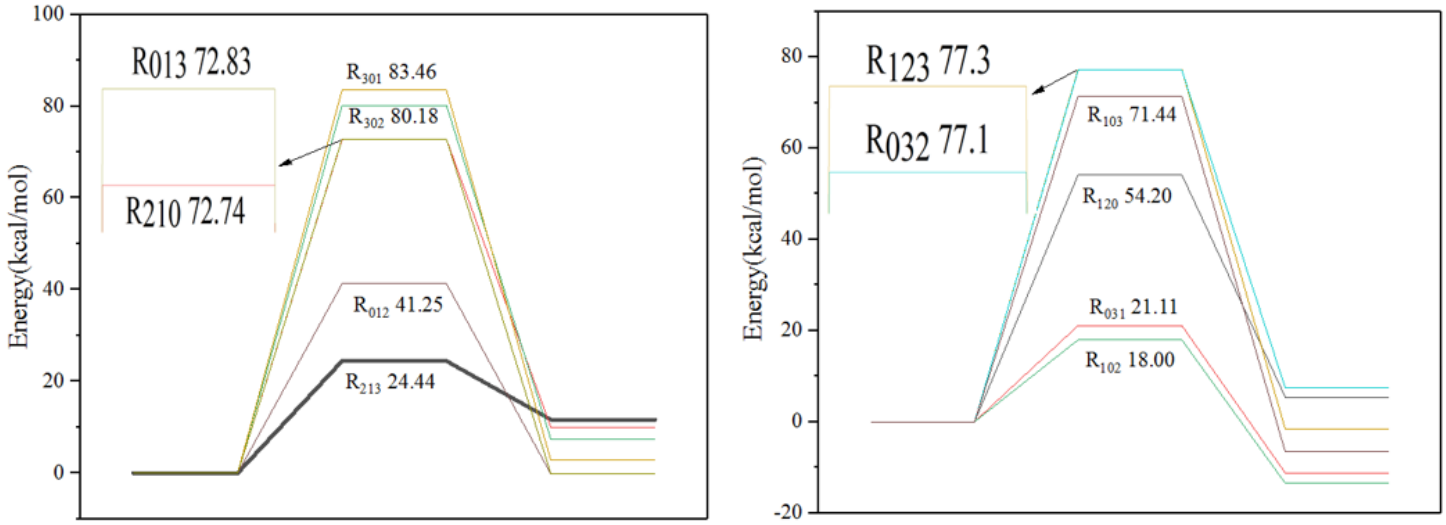

Figure 10

Energy profiles of the third hydrogenation step on Pt/Mo2C(001) (left) and Mo2C(001) (right) surfaces

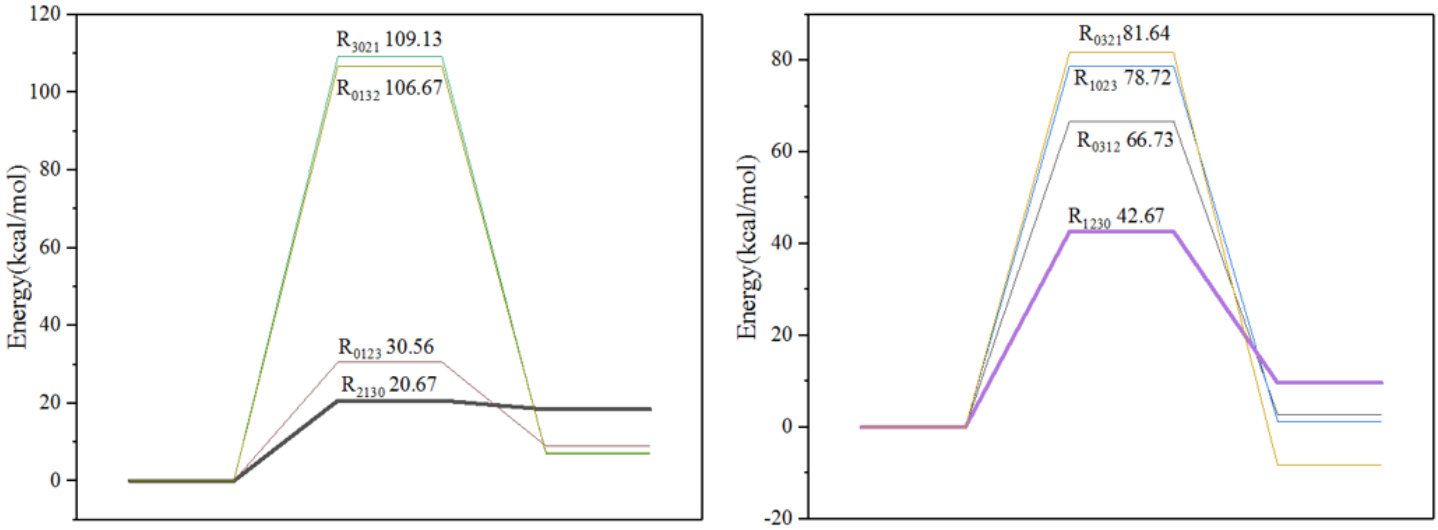

Figure 11

Energy profiles of the forth hydrogenation step on Pt/Mo2C(001) (left) and Mo2C(001) (right) surfaces